JTTEE5 18:490–499
DOI: 10.1007/s11666-009-9379-1
1059-9630/$19.00 © ASM International



# Jetting-Out Phenomenon Associated with Bonding of Warm-Sprayed Titanium Particles onto Steel Substrate

*KeeHyun Kim, Makoto Watanabe, and Seiji Kuroda*

*(Submitted May 28, 2009; in revised form July 23, 2009)*

**Titanium powder particles accelerated and simultaneously heated by the supersonic gas flow were deposited onto steel substrate by the warm spraying process. The sprayed particles were heavily deformed and bonded to the substrate in solid state. Especially, all the deposited particles showed jetting-out of materials out of the particle-substrate interface triggered by the adiabatic shear instability known to occur under such shock impact conditions. High-magnified images showed that grain refinement occurred in the jetting-out region by dynamic recrystallization. Furthermore, the elemental analysis using the electron energy loss spectrum showed jetting-outs of the substrate as well as the particle. Numerical simulation based on the Johnson-Cook plastic deformation model showed that the jetting-out phenomenon commences about 10 ns after the initial contact of the particle with the substrate and at a position away from the center bottom of particle, where the highest compressive stress is experienced.**

**Keywords** bonding mechanism, dynamic recrystallization, grain refinement, jetting-out, warm spraying

## 1. Introduction

In the coating processes such as cold spraying (Ref 1-10) and warm spraying (Ref 11-13), metallic powder particles accelerated by a supersonic gas flow are deposited onto a suitable substrate in solid state. The impact of sprayed particles with high velocity exceeding a critical value onto the substrate forms bond between the particle and the substrate. The bonding mechanism, however, has been a topic of many discussions in the fields (Ref 1-8). It is well known that the so-called adiabatic shear instability, which means local domination of thermal softening over work hardening associated with a discontinuous jump in strain, temperature, and an immediate breakdown of stress, can result in the bonding between sprayed particle and substrate. If the shear instability occurs, the oxide covering on the surface of the particle as well as the substrate can be broken-up due to the mighty jetting-out of the particle upon impact on the substrate. Such jetting-out usually occurs upon high-velocity impact of a projectile against a target and extrudes the projectile at the surface of contact (Ref 14). In the warm spraying process, the jetting-out can create thin rims around the deposited particle (Ref 15). As a result, the metallurgical bonding between the particle and the substrate can be formed. Although many studies based on this shear instability and the breaking-up of oxide have been made so far, there is little on the microstructural features in the jetted-out region as well as the role of jetting-out in the bonding mechanism.

The warm spray process developed in our group can make relatively dense coatings of various metals with low oxidation at one of the most suitable spraying conditions (Ref 11-13). In the process, spraying powders accelerated by a supersonic jet are impacted and heavily deformed on a substrate. Especially, the sprayed particles can be deposited in solid state due to inert gas such as nitrogen mixed to lower the temperature of the supersonic gas flow generated by the combustion of kerosene and oxygen. In this study, the jetting-out phenomenon of particles impacting on a substrate via the warm spraying process was investigated in detail. Especially, only single titanium particles were deposited on steel substrate to avoid distortions induced by accumulation of deposited particles.

## 2. Experimental

### 2.1 Feedstock Material, Spraying Process, and Conditions

Commercially available spherical titanium powder (TILOP-45 μm, Sumitomo Titanium Corporation, Tokyo, Japan) was sprayed on a mirror-polished steel substrate (JIS: S45C, Fe-0.45 mass% C) to investigate the jetting-out phenomenon of particles impacted on the substrate. Moreover, single layer of titanium particles was deposited

This article is an invited paper selected from presentations at the 3rd Asian Thermal Spray Conference (ATSC2008) and has been expanded from the original presentation. ATSC2008 was held at Nanyang Executive Centre, Singapore, November 6-7, 2008, and chaired by K.A. Khor.

**KeeHyun Kim, Makoto Watanabe,** and **Seiji Kuroda**, Hybrid Materials Center, National Institute for Materials Science (NIMS), 1-2-1 Sengen, Tsukuba, Ibaraki 305-0047, Japan. Contact e-mail: kim.keehyun@nims.go.jp.

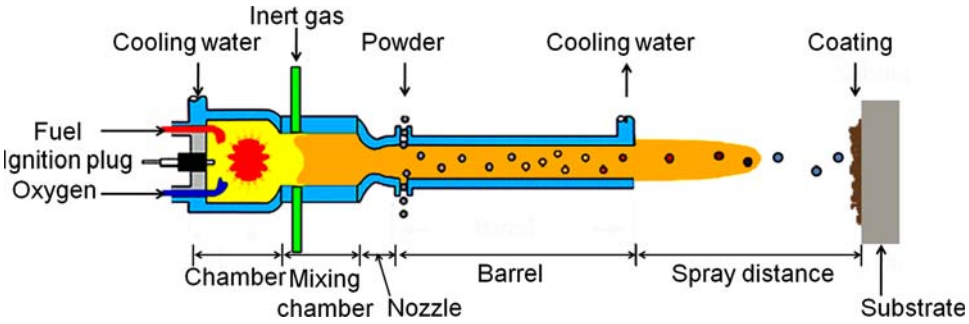


**Fig. 1** Schematic diagram of warm spraying equipment

**Table 1 List of spray parameters**

| Parameter | Unit | Value |
|---|---|---|
| Fuel flow rate | $dm^3$/min | 0.30 |
| Oxygen flow rate | $dm^3$/min | 623 |
| Nitrogen flow rate | $dm^3$/min | 1500 |
| Barrel length | mm | 200 |
| Spray gun traverse velocity | mm/s | 1500 |
| Spraying distance | mm | 180 |
| Powder feed rate | g/min | 4 |
| Powder feed gas | ··· | Nitrogen |
| Substrate temperature | °C | 25 |

to avoid distortions induced by accumulation of deposited particles via the warm spraying process. Figure 1 shows a schematic diagram of warm spraying equipment, which has been modified from a commercial high-velocity oxy-fuel (HVOF) spray apparatus (Ref 13). In the process, the combustion of fuel generates a supersonic gas flow but contrary to the conventional HVOF process, the gas flow is mixed with nitrogen in a mixing chamber to lower its temperature. Then, feed-stock powder is fed into the barrel and accelerated and simultaneously heated by the temperature-controlled gas flow. Consequently, by varying the temperature of particles at the impact in a wider range, the process can control effectively the microstructure of sprayed coatings. When used for highly reactive metals such as titanium, for example, it is capable of attaining highly dense coatings without causing excessive oxidation. In this study, the spray distance was set at 180, 380, and 580 mm, and the nitrogen flow rate was 1500 $dm^3$/min, which can avoid melting of sprayed powder (Ref 13). The detailed spray parameters are summarized in Table 1.

### 2.2 Microstructure Observation and Transmission Electron Microscopy Sample Preparation

The as-deposited titanium particles were, first, observed by a field emission scanning electron microscope (FE-SEM, JEOL JSM-6500). Then, the deposited particles were cross-sectioned and polished by standard metallographic techniques to reveal a transverse section and observed by FE-SEM. Backscattered electron (BSE) images and energy dispersive x-ray spectroscopy (EDX) were also obtained on the samples. The thin sample for the transmission electron microscopy (TEM) observation was exquisitely made by the focused ion beam (FIB) lift-out procedure at the desired region using Hitachi FB-2000. The detailed sampling procedure was explained elsewhere (Ref 13, 16). The high-magnified images were acquired by a normal TEM (JEOL JEM 2000FX) operated at 200 kV, and STEM (JEOL JEM 2500SES) coupled with an electron energy loss (EEL) spectrometer (Gatan Enfina).

### 2.3 Numerical Modeling

In the warm spraying process, which uses impacts of in-flight particles with very high velocity above 700 m/s at an optimized spraying condition for titanium, the impact-induced development of strain, stress, and temperature fields near the impacted region is very fast. Therefore, the modeling of particle impact was carried out by using a commercial finite element code (ABAQUS/explicit version 6.5) and the Johnson-Cook plasticity model was used to estimate the evolution of strain, stress, and temperature distributions near the impacted region (Ref 2, 3, 6, 17-19). An axisymmetric analysis model was used (Ref 19), in which a titanium particle with radius of 28 μm, velocity at 760 m/s, and temperature 1100 K was impacted on the steel substrate. The Johnson-Cook model including strain hardening, strain-rate hardening, and thermal softening effects can be written as follows (Ref 17-19):

$$\sigma = [A + B\varepsilon^n][1 + C\ln\dot{\varepsilon}]\left[1 - \left(\frac{T - T_r}{T_m - T_r}\right)^m\right]$$

where σ denotes the equivalent tensile flow stress, ε the equivalent plastic strain, $\dot{\varepsilon}$ the normalized plastic strain rate, $T_r$ the room temperature, $T_m$ the melting point, and $A$, $B$, $C$, $m$, and $n$ are constants and given in Table 2. For titanium and medium-carbon steel S45C, constant $m$ is 1 and 0.55 (Ref 17, 20), respectively. In this study, most of the parameters were set as temperature dependent values based on the literatures (Ref 17-20).

## 3. Results and Discussion

### 3.1 SEM Observation of Deposited Titanium Particles

Figure 2 shows SEM images of as-received and deposited titanium particles, so-called splats, at different

spraying distances. The temperature and velocity of sprayed titanium particles calculated by the gas dynamics simulation showed that as the distance increases, the temperature and velocity of in-flight particles decrease (Ref 13), i.e., at 180 mm, which is an optimized spraying distance for titanium in warm spraying, about 760 m/s and 1100 K, at 380 mm about 650 m/s and 900 K, and at 580 mm (extrapolated) about 450 m/s and 650 K, respectively. As shown in Fig. 2, the amount of deposited splats dramatically decreased. In a measured area of about 240 μm × 180 μm of Fig. 2, which was the center region of spraying gun, the number of deposited splats was 29 at 180 mm, 7 at 380 mm, and only 1 at 580 mm because the driving force to make the deposition decreases as the spraying distance increases even though the spreading of the sprayed particles' flux could have an effect on the number. Figure 3 is the detailed images of deposited splats at the various viewing angles. The splats were highly deformed in solid state (Ref 13). Especially, the jetting-out of titanium was recognized as indicated by arrows in the Fig. 3. It is obvious that in Fig. 3(c) the particle sprayed at 580 mm also showed the jetting-out even though the total number of deposited splat was very small at the spraying distance. Furthermore, as already shown in Fig. 2, all the deposited particles showed the jetting-out regardless of the spraying distance. It means that the jetting-out of deposited particle is indispensable to make the deposition of sprayed particle. Similarly, in cold spraying process, the jet formation is required for successful bonding (Ref 6, 21).

**Table 2 Johnson-Cook parameters used in finite element model for room temperature case**

| Parameter | Ti | S45C |
|---|---|---|
| Yield stress ($A$), MPa | 480 | 175 |
| Strength coefficient ($B$), MPa | 1352 | 380 |
| Strain rate coefficient ($C$) | 0.04 | 0.06 |
| Strain hardening exponent ($n$) | 0.27 | 0.32 |
| Melting temperature, K | 1941 | 1809 |
| Reference temperature, K | 293 | 293 |
| Reference strain rate, 1/s | 1 | 1 |

In this study, most of the parameters were set as temperature-dependent values based on handbooks

### 3.2 TEM Observation and Element Distributions in the Jetting-Out Region

Figure 4 shows a typical vertical cross-sectional TEM image. The deposited splat clearly shows the jetting-out phenomenon. Furthermore, very fine grains are formed at the jetting-out region, as indicated by discontinuous multiple rings in selected area diffraction patterns in Fig. 4(b). The grain refinement could be made by dynamic recrystallization (Ref 15). As soon as the sprayed titanium particle impacts on the substrate, it is heavily deformed and resulted in the adiabatic shear instability, i.e., a

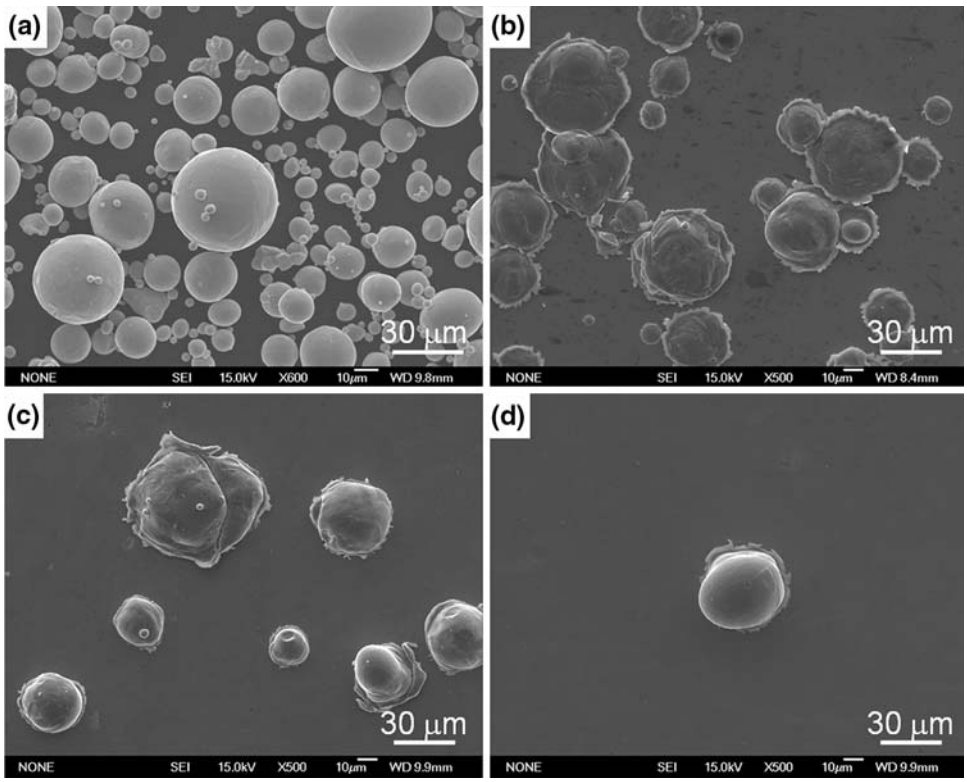


**Fig. 2** SEM images of as-received and deposited titanium particles at different spray distances: (a) as-received, (b) 180 mm spray distance, (c) 380 mm, and (d) 580 mm

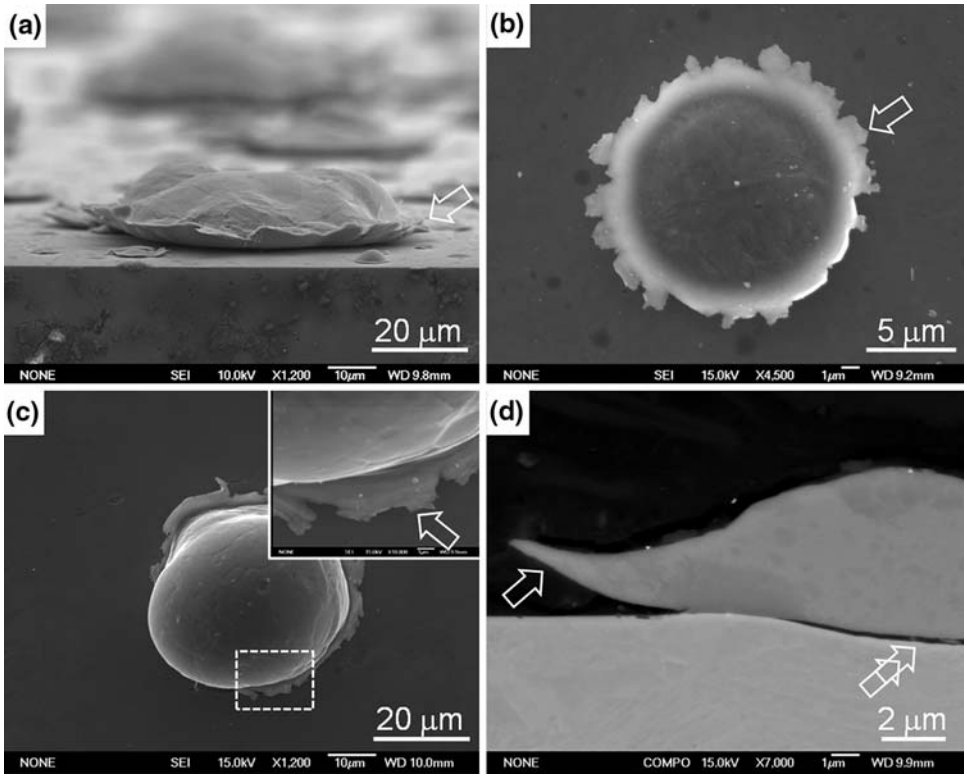


**Fig. 3** SEM image of titanium splat showing the jetting-out: (a) 20° tilting view, (b) top view of single splat sprayed at 180 mm, (c) top view of a splat sprayed at 580 mm, and (d) typical cross-sectional image of single splat. The arrow in each panel indicates the jetting-out of titanium. The inset image in (c) is a magnified image of the boxed area

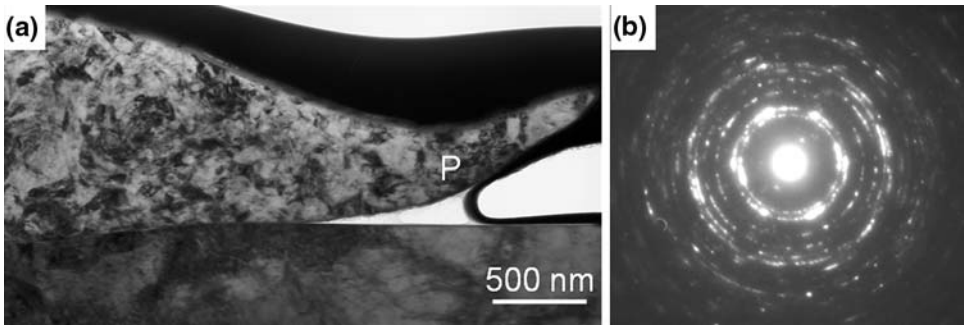


**Fig. 4** Typical cross-sectional TEM image (a) and selected area diffraction patterns at the jetted out region marked with P (b). The upper black layer on the splat is a protective tungsten layer deposited during the TEM sample preparation using the FIB

discontinuous jump in strain, temperature, and an immediate breakdown of stress. Consequently, the strain and temperature rise can trigger the recrystallization of heavily deformed grains during the impact without any post-heat treatment.

Figure 5 shows a TEM image (a), a STEM image at the marked region of (a), and an electron energy loss spectrum (EELS) line profile along the dotted line of (b) near the interface of another titanium splat and substrate at a spraying distance of 180 mm. As shown in Fig. 5(c), the elemental analysis using EELS on the side of titanium near the jetting-out region shows that the amount of titanium on the bottom surface of the jetted-out part of the splat is quite low compared to iron and oxygen, which indicates clearly that the jetting-out of iron from the substrate occurred and resulted in the iron attached on the bottom surface of the splat. It means that the jetting-out induced by the very strong impact of sprayed particle can have an effect on the substrate itself as well as the particle.

To investigate the jetting-out phenomenon of substrate, the surface of a steel substrate with the size of $10 \times 10 \times 5$ mm$^3$ was coated with gold of about 30 nm

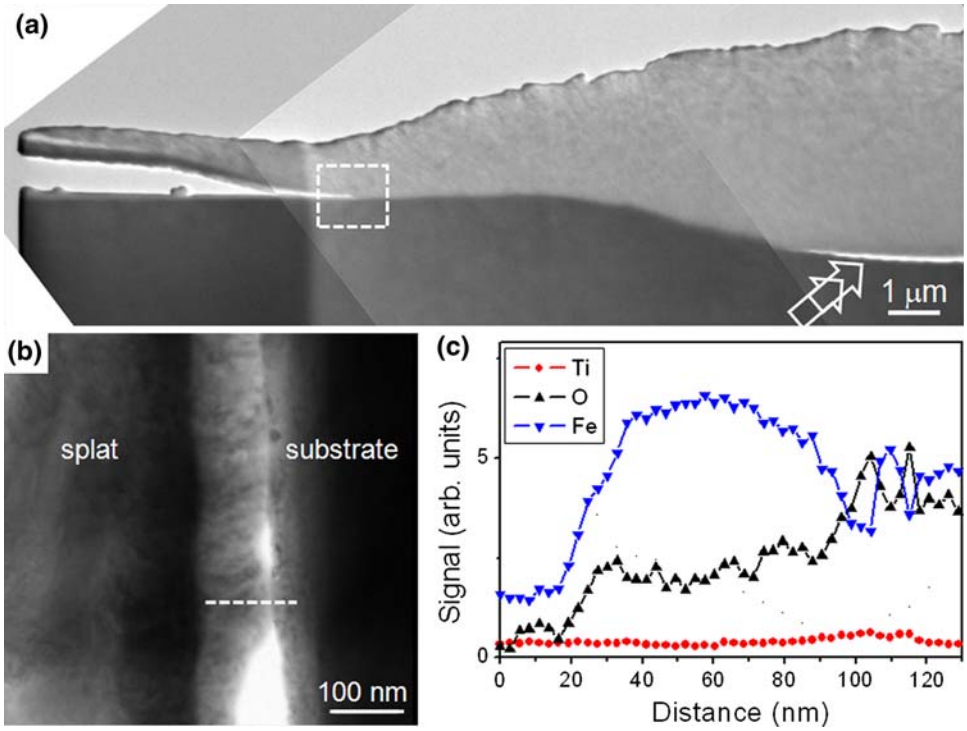


**Fig. 5** TEM image and elemental analysis of single titanium splat: (a) low magnification image by TEM, (b) STEM image at the marked region of (a), and (c) EELS line profile along the dotted line of (b)

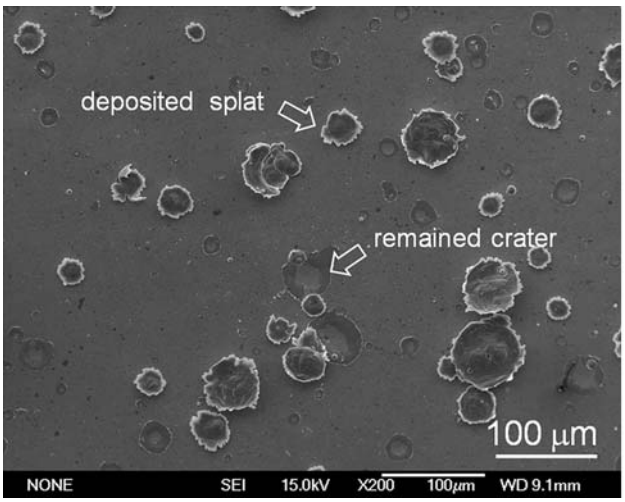


**Fig. 6** Top view of the SEM image of deposited titanium particles on gold-coated steel substrate

thickness prior to spraying. Other spraying conditions were kept unchanged except the gold-coated substrate. Figure 6 shows SEM images of titanium splats deposited onto the gold-coated substrate. Contrary to the result of titanium splats on the mirror-polished substrate, some craters left by the bounced-off particles were recognized as shown in the figure. SEM-EDX mappings (Fig. 7) near a crater left on the gold-coated substrate showed clearly that the gold film was removed only in the outer ring region except the center region. In addition, as shown in Fig. 7(d), some peeled-off gold films indicate that the jetting-out of gold occurred in solid state and in the outward direction. It means that the jetting-out occurred not only out of the titanium particle but also out of the gold film, which is much more deformable as compared to steel. It is believed that some particles which jetted out only the gold film layer with about 30 nm thickness but did not jet out the steel substrate beneath were bounced off. The results suggest that huge shear deformation by jetting-out can create large area of the fresh (or highly active) metal surface by breaking the oxides naturally formed on the substrate and the ones on the particle, which is indispensable to induce intimate bonding between the sprayed metallic particle and the metallic substrate, both of which are usually covered with some oxide.

### 3.3 Numerical Simulation on the Jetting-Out Phenomenon

As mentioned in the previous section, it is clear that the jetting-out of gold film occurred only at the outer region. Figure 8 shows the equivalent plastic strain history developed at several nodes in a titanium particle, which is estimated by FEM analysis. In nodes A and B, the strains dramatically increased as the impact time increased, while the strains at nodes C and D gradually increased. The abrupt increase is related to the adiabatic

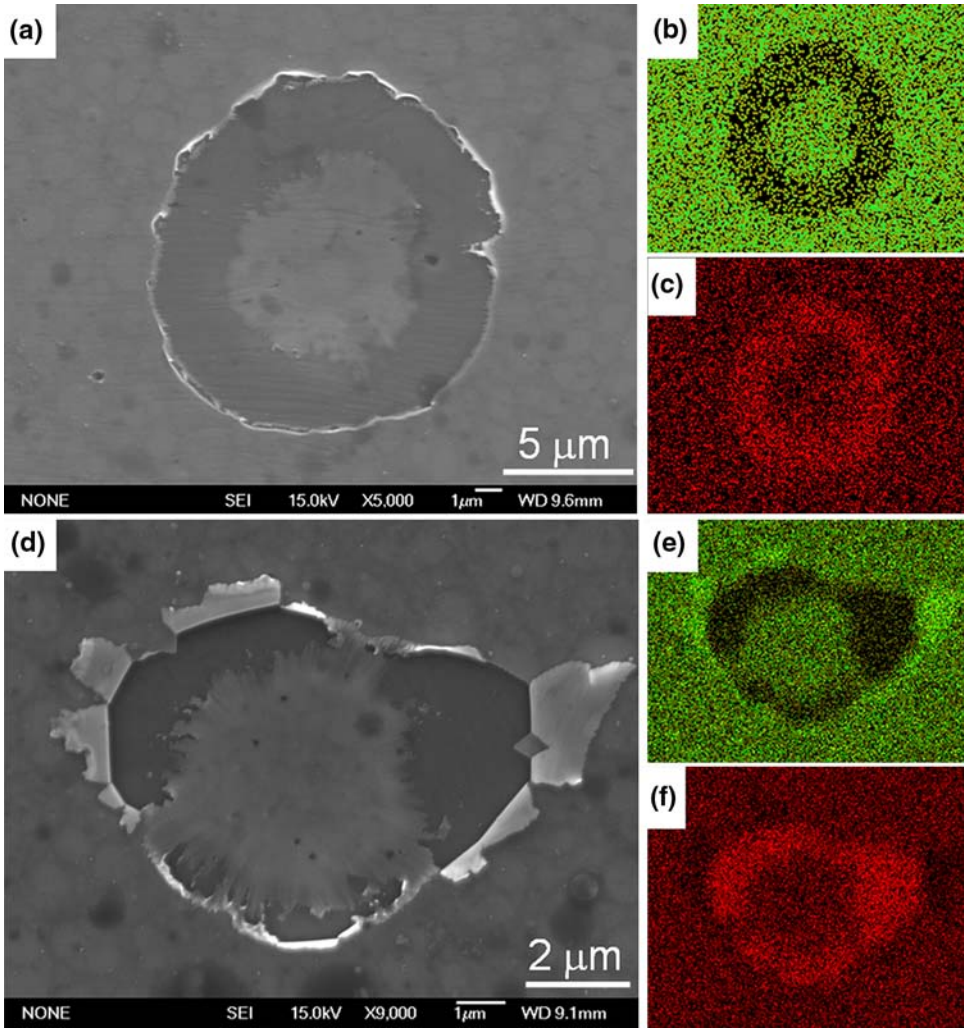


**Fig. 7** Crater left on gold-coated substrate by a bounced-off particle: (a, d) SEM image, (b, c, e, f) SEM-EDX mapping of gold (b, e), and iron (c, f)

shear instability in the region. Furthermore, Fig. 8 clearly shows that the instability commences at a position (near the node B in this study) away from the bottom center. We believe that the regions, i.e., the gold jetting-out region in Fig. 7 and the node B in Fig. 8, correspond to the area where the vigorous shear instability of titanium particle occurred.

Figure 9 shows the shape of a titanium particle estimated by FEM, which shows that after about 10 ns the jetting-out phenomenon commences at the position where the strain is dramatically increased as shown in Fig. 8. The jetting-out commencing time depending on the material properties can be short or long according to the combination of particle and substrate (Ref 22). These results based on the Johnson-Cook plastic deformation model clearly showed that the jetting-out phenomenon resulting from the shear instability takes place at about 10 ns after the initial contact of the titanium particle with the steel substrate. Moreover, the jetting-out commences at a position away from the bottom center.

### 3.4 The Importance of Jetting-Out Phenomenon

As shown in Fig. 2 and 3, all the deposited splats showed the jetting-out phenomenon. However, if we see Fig. 3(d) and 5(a) carefully again (see the double arrow in each figures), there is a void between the center bottom of titanium and the substrate. Furthermore, in Fig. 6 and 7, gold in the center region of the left craters was not jetted-out but remained. Figure 10 shows the estimated stress evolution after the impact. The numerical simulation showed that, in nodes R and S, as soon as the sprayed particle impacts onto the substrate, huge compressive stress were developed. However, the stress was changed to tensile as the impact time goes up. The maximum tensile stress for the particle velocity of 760 m/s and temperature of 1100 K could reach up to about 800 MPa at the epicenter. The high tensile stress in the titanium particles' region can detach the titanium from the substrate. Furthermore, the numerical simulation implies that the debonding at the center bottom of

splat induced by the tensile stress, as indicated by an arrow in Fig. 10, could occur at about 75 ns after the particle impact on the substrate in this study. Therefore, the results suggest that the jetting-out occurred first, i.e., after 10 ns, and formed the bonding between the splat and the substrate at a position, i.e., at node B, away from the center bottom of sprayed particle where the highest compressed stress is experienced. Then, the rebounding phenomenon could be initiated at about 75 ns if the bonding was not strong enough. The jetting-out and rebounding procedure based on the results of numerical simulation was schematically depicted in Fig. 11.

The typical cross-sectional image of a deposited splat and the crater left on a gold-coated substrate were compared as shown in Fig. 12. Interestingly, the rebounded region and the gold remained region were well matched. In addition, the bonded region and the gold jetted-out region were also very well matched. Therefore, it means that the intimate bonding of the particle and the substrate can be formed in the region where jetting-out induced by shear instability occurs. Figure 12 also shows that the

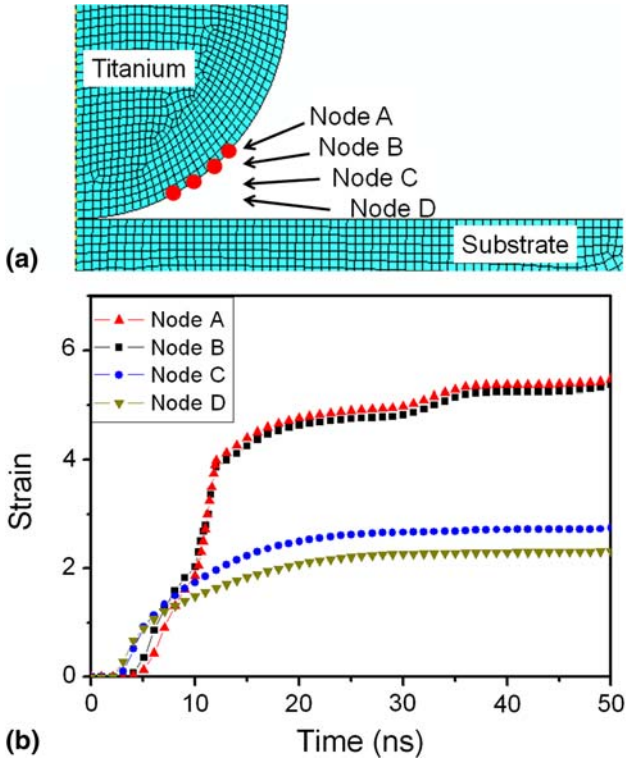


**Fig. 8** Developed strain history estimated by numerical simulation using FEM: (a) selected nodes and (b) estimated strain history after impact

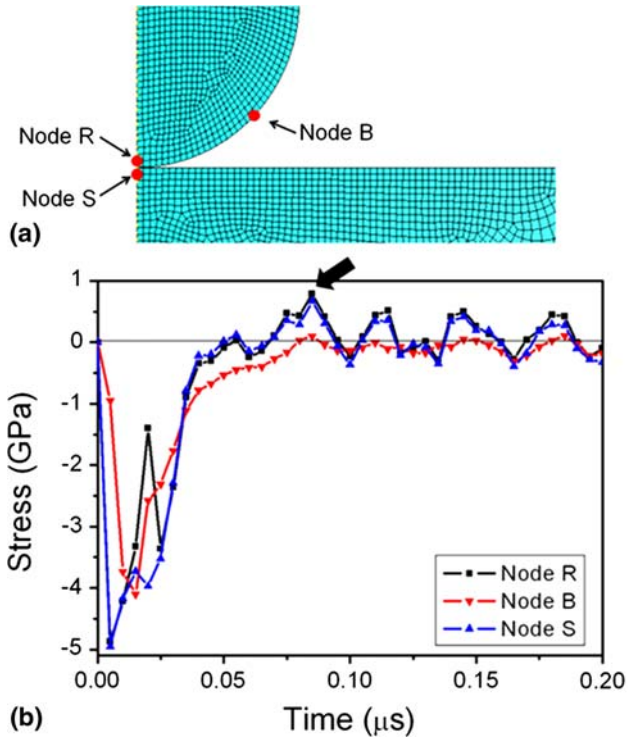


**Fig. 10** Finite-element modeling: (a) model and (b) estimated stress evolution after the impact. The arrow in (b) indicates the maximum tensile stress

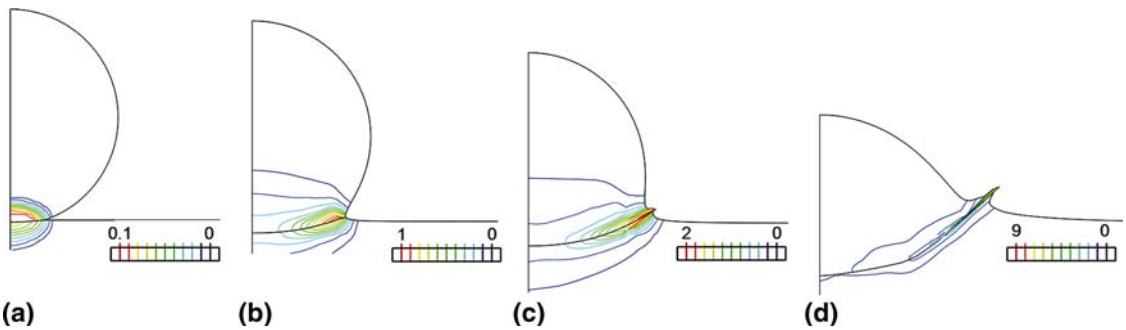


**Fig. 9** Sequence of shape change of a titanium particle calculated by FEM: (a) 1 ns after impact, (b) 5 ns, (c) 10 ns, and (d) 100 ns. The colored lines indicate the magnitude of equivalent plastic strain

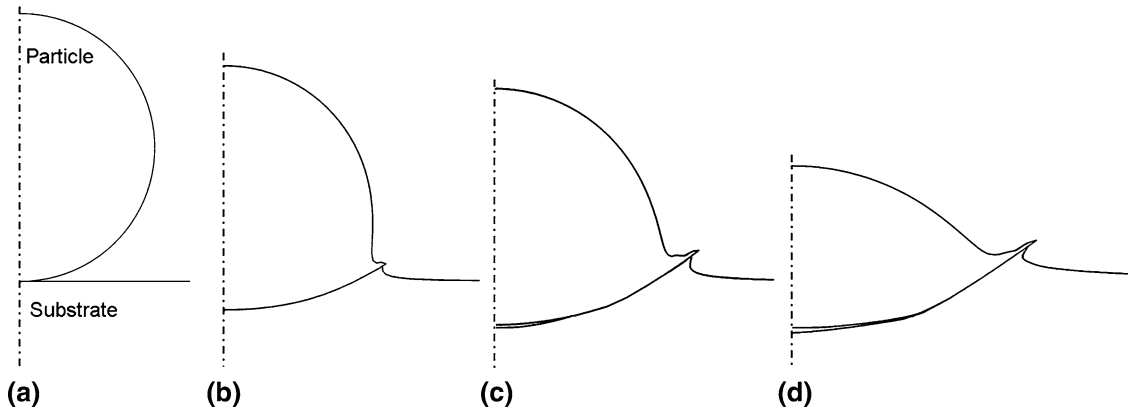


**Fig. 11** Schematic diagram of bonding mechanism of single metallic powder: (a) before impact, (b) 10 ns after impact, (c) after 30 ns, and (d) after 100 ns

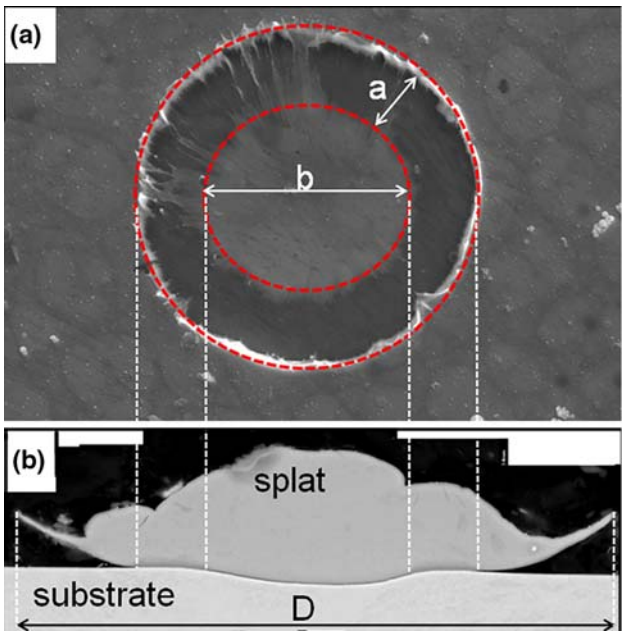


**Fig. 12** Comparison of one crater left by a bounced-off particle and one typical cross-sectional SEM image of a deposited titanium particle

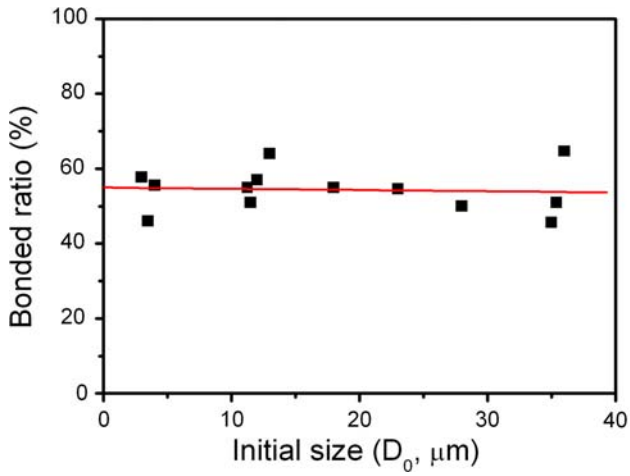


**Fig. 13** Dependence of bonded ratios of the deposited titanium particles on steel substrate

bonding between the particle and the substrate did not occur in the whole interfacial region. The bonding ratio (BR) was simply defined as follows:

$$\mathrm{BR} = \left\{\pi(a+0.5b)^2 - \pi(0.5b)^2\right\} \Big/ \left\{\pi(a+0.5b)^2\right\}$$

where $a$ and $b$ are indicated in Fig. 12, and for simplicity, the bonded and the rebounded region were assumed as circles. The initial particle diameter ($D_0$) of each splat could be estimated from the diameter measurement of deposited particles and expressed as follows (Ref 23):

$$D_0 = 0.53D + 0.05$$

where $D$ is the diameter of deposited splat in Fig. 12. As shown in Fig. 13, the bonded ratio is about 55% and nearly constant regardless of the initial powder size. The findings in this study can be summarized that in the warm spraying of titanium onto steel substrate, even though all the deposited particles showed the jetting-out phenomenon, intimate bonding between the particles and substrate was formed at only 55% of the whole interfacial area, which should be overcome to make much more strongly bonded coating layer by the warm spraying process.

We must note that although the jetting-out phenomenon occurred on gold-coated substrate (see Fig. 6, 7), many particles were not bonded to the substrate but bounced off. In the case of the titanium particles sprayed onto a mirror-polished steel substrate, the deposition efficiency is above 99% (Ref 23). It means that nearly all sprayed titanium particles can be deposited on the clean steel substrate. However, on the gold-coated steel substrate, the deposition efficiency is only 40 to 50% even though the jetting-out occurred. It may be for this reason that, in the bounced-off case, the steel substrate located

beneath the gold layer might not be deformed or jetted-out because on gold-coated substrate the jetting-out occurred only in the thin gold coating layer itself and the bonding strength between the gold layer and the steel substrate was weak and thus the substrate could not follow the deformation of the gold surface layer during jetting-out. Consequently, the oxide covered on the surface of the steel substrate might not be sufficiently removed to form the bonding of titanium in the particle and iron in the substrate, which remains as a matter to be discussed further. However, compared with the intimate bonding formed between titanium particles and the mirror-polished steel substrate (Ref 16), it is clear that the bonding between the particles and the substrate can be prohibited by a gold coating layer located between the particles and the steel substrate.

## 4. Conclusion

Titanium powder particles accelerated and simultaneously heated by the warm spraying process were heavily deformed and bonded to steel substrate in solid state. All deposited particles showed the jetting-out triggered by the shear instability. TEM observation in the jetted-out region showed that very fine grains were formed by the dynamic recrystallization. Furthermore, the elemental analysis using EELS revealed the jetting-out of the iron existing in the substrate as well as the titanium particle. On the gold-coated substrate, many titanium particles were bounced off and left some craters. From the traces, the jetting-out phenomenon of substrate was clearly recognized. Numerical simulation showed that the jetting-out phenomenon of titanium particle and steel substrate takes place at about 10 ns after the initial contact of the titanium particle with the steel substrate. Moreover, the jetting-out commences at a position away from the center bottom of a titanium splat, which is the most highly compressed point. Finally, the results suggested a sequence of jetting-out and deposition mechanism of warm-sprayed single titanium particle onto steel substrate. As soon as the sprayed particles make contact with the substrate, the mirror-polished or the gold-coated substrate as well as the particle are heavily compressed. The strong compressive stress generates the resultant shear stress and it accelerates laterally at the interface of the particle and the substrate, which can trigger strong shear straining as well as locally dominant thermal softening. As the resistance of material against the shear flow is low in the thermally softened region, the material loses its shear strength and undergoes excessive deformation. Consequently, the jetting-out phenomenon occurs, which can jet out the steel substrate or the gold-coated layer as well as the particle.

In the warm spraying of titanium particles onto the mirror-polished steel substrate, intimate bonding between the particles and the substrate can be formed by the jetting-out phenomenon; however, the bonded region is 55% of the whole interfacial area.

## Acknowledgment

The authors would like to acknowledge Dr. K. Mitsuishi and Dr. K. Iakoubovskii of NIMS for the EELS analysis and Ms N. Kawano, Mr M. Komatsu, and Mr N. Kakeya of NIMS for sample preparations. This research was supported by the Nanotechnology Network program and World Premier International Research Center Initiative on Materials Nanoarchitectonics of MEXT, Japan and KAKENHI 19360335.

## References

1. R.C. Dykhuizen, M.F. Smith, D.L. Gilmore, R.A. Neiser, X. Jiang, and S. Sampath, Impact of High Velocity Cold Spray Particles, *J. Therm. Spray Technol.*, 1999, **8**(4), p 559-564
2. M. Grujicic, J.R. Saylor, D.E. Beasley, W.S. DeRosset, and D. Helfritch, Computational Analysis of the Interfacial Bonding Between Feed-Powder Particles and the Substrate in the Cold-Gas Dynamic-Spray Process, *Appl. Surf. Sci.*, 2003, **219**(3-4), p 211-227
3. H. Assadi, F. Gärtner, T. Stoltenhoff, and H. Kreye, Bonding Mechanism in Cold Gas Spraying, *Acta Mater.*, 2003, **51**(15), p 4379-4394
4. T.V. Steenkiste and J.R. Smith, Evaluation of Coatings Produced via Kinetic and Cold Spray Processes, *J. Therm. Spray Technol.*, 2004, **13**(2), p 274-282
5. C. Borchers, F. Gärtner, T. Stoltenhoff, and H. Kreye, Microstructural Bonding Features of Cold Sprayed Face Centered Cubic Metals, *J. Appl. Phys.*, 2003, **93**(8), p 4288-4292
6. T. Schmidt, F. Gärtner, H. Assadi, and H. Kreye, Development of a Generalized Parameter Window for Cold Spray Deposition, *Acta Mater.*, 2006, **54**(3), p 729-742
7. T. Marrocco, D.G. McCartney, P.H. Shipway, and A.J. Sturgeon, Production of Titanium Deposits by Cold-Gas Dynamic Spray: Numerical Modeling and Experimental Characterization, *J. Therm. Spray Technol.*, 2006, **15**(2), p 263-272
8. T. Hussain, D.G. McCartney, P.H. Shipway, and D. Zhang, Bonding Mechanisms in Cold Spraying: The Contributions of Metallurgical and Mechanical Components, *J. Therm. Spray Technol.*, 2009, **18**(3), p 364-379
9. A. Papyrin, V. Kosarev, S. Klinkov, A. Alkhimov, and V. Fomin, *Cold Spray Technology*, Elsevier, Amsterdam, 2007
10. V.K. Champagne, *The Cold Spray Materials Deposition Process*, Woodhead Publishing/CRC Press, Cambridge, 2007
11. S. Kuroda, J. Kawakita, M. Watanabe, and H. Katanoda, Warm Spraying—A Novel Coating Process Based on the High-Velocity Impact of Solid Particles, *Sci. Technol. Adv. Mater.*, 2008, **9**(3), 033002 (17 pp)
12. J. Kawakita, S. Kuroda, T. Fukushima, H. Katanoda, K. Matsuo, and H. Fukanuma, Dense Titanium Coatings by Modified HVOF Spraying, *Surf. Coat. Technol.*, 2006, **201**(3-4), p 1250-1255
13. K.H. Kim, M. Watanabe, J. Kawakita, S. Kuroda, Effects of Temperature of In-flight Particles on Bonding and Microstructure in Warm Sprayed Titanium Deposits, *J. Therm. Spray Technol.*, 2009, **18**(3), p 392-400
14. S.W. Kieffer, Droplet Chondrules: Jetting on High-Velocity Collision of Small Meteoritic Particles May Have Produced Droplet Chondrules, *Science*, 1975, **189**(4200), p 333-340
15. K.H. Kim, M. Watanabe, J. Kawakita, and S. Kuroda, Grain Refinement in a Single Titanium Powder Particle Impacted at High Velocity, *Scripta Mater.*, 2008, **59**(7), p 768-771
16. K.H. Kim, M. Watanabe, K. Mitsuishi, K. Iakoubovskii, and S. Kuroda, Impact Bonding and Rebounding Between Kinetically Sprayed Titanium Particle and Steel Substrate Revealed by High Resolution Electron Microscopy, *J. Phys. D: Appl. Phys.*, 2009, **42**, 065304 (5 pp)
17. G.R. Johnson, Material Characterization for Warhead Computations, *Prog. Astronaut. Aeronaut.*, 1993, **155**, p 165-197

18. S. Seo, O. Min, and H. Yang, Constitutive Equation for Ti-6Al-4V at High Temperatures Measured Using the SHPB Technique, *Int. J. Impact Eng.*, 2005, **31**, p 735-754
19. K. Yokoyama, M. Watanabe, S. Kuroda, Y. Gotoh, T. Schmidt, and F. Gärtner, Simulation of Solid Particle Impact Behavior for Spray Processes, *Mater. Trans.*, 2006, **47**(7), p 1697-1702
20. *ASM International Handbook, vol. 8, Mechanical Testing and Evaluation*, Materials Park, OH, 2000
21. C. Borchers, T. Schmidt, F. Gärtner, and H. Kreye, High Strain Rate Deformation Microstructures of Stainless Steel 316L by Cold Spraying and Explosive Powder Compaction, *Appl. Phys. A*, 2008, **90**, p 517-526
22. M. Grujicic, C.L. Zhao, W.S. DeRosset, and D. Helfritch, Adiabatic Shear Instability Based Mechanism for Particles/Substrate Bonding in the Cold-Gas Dynamic-Spray Process, *Mater. Des.*, 2004, **25**(8), p 681-688
23. K.H. Kim, M. Watanabe, and S. Kuroda, Thermal Softening Effect on the Deposition Efficiency and Microstructure of Warm Sprayed Metallic Powder, *Scripta Mater.*, 2009, **60**(8), p 710-713